

1 A laboratory investigation of bed-load transport of gravel sediments under 2 dam break flow

3 Khabat Khosravi*¹, Amir H. N Chegini*², James R. Cooper³, Prasad Daggupati¹, Luca Mao⁴, Andrew
4 Binns¹, Mahmood Habibnejad⁵, Kaka Shahedi⁵

5 ¹ School of Engineering, University of Guelph, Ontario, Canada.

6 ² School of the Built Environment, Heriot-Watt University, Edinburgh Campus, Edinburgh EH144AS, UK.

7 ³ Department of Geography and Planning, School of Environmental Sciences, University of Liverpool, Liverpool L69 7ZT, UK.

8 ⁴ School of Geography, University of Lincoln, Lincoln, UK.

9 ⁵ Sari Aricultural Science and Natural Resources University, Sari, Iran

10

11 *Corresponding Authors: Khabat Khosravi (khabat.khosravi@gmail.com) and Amir Chegini (ahnchegini@yahoo.co.uk).

12

13 Abstract

14 Dam break flows and resulting river bed erosion can have disastrous impacts on human safety,
15 infrastructure, and environmental quality. However, there is a lack of research on the mobility of
16 non-uniform sediment mixtures resulting from dam break flows and how these differ from
17 uniform sized sediment. In this paper, laboratory flume experiments revealed that coarse and fine
18 fractions in non-uniform sediment had a higher and a lower bed-load parameter, respectively,
19 than uniform sediments of the same size. Thus, the finer fractions were more stable and the
20 coarser fractions more erodible in a non-uniform bed compared to a uniform-grained bed. These
21 differences can be explained by the hiding and protrusion of these fractions, respectively. By
22 investigating changes in mobility of the mixed-size fractions with reservoir water levels, the
23 results revealed that at low water levels, when the coarser fractions were only just mobile, the
24 bed-load parameter of the finer fractions was higher than the coarser fractions. The opposite was
25 observed at a higher water level, when a significant proportion of the coarsest fractions were
26 mobilized. The higher protrusion of these grains had an important effect on their mobility
27 relative to the finer grains. The transported sediment on these mixed-sized beds was coarser than
28 the initial bed sediment, and became coarser with an increase in reservoir water level.

29 **Key words:** dam break, bed-load transport, gravel, laboratory flume

30 **Introduction**

31 Dams have been constructed all over the world to provide water supply for drinking, agriculture,
32 industry, and power generation; they are also a key component of flood defense. However, when
33 they collapse, the resulting floods can have disastrous impacts on infrastructure, human safety,
34 and environmental quality. Dam breaks can take place due to overtopping, piping, slope
35 instability, insufficient spillway capacity and earthquakes (Molu 1995; Bozkus 2004). Future
36 changes in climate, particularly in terms of storm severity, are likely to increase the risk of dam
37 failure as the majority of existing structures were designed based on past and current hydro-
38 climatological conditions (Soares-Frazão et al. 2012).

39 Damage to infrastructure from sediment erosion and deposition can be as severe as the impact of
40 the flood wave itself (Spinewine & Zech, 2007). The intensity of sediment transport close to the
41 dam can be such that the rate of sediment transport is similar to the rate of water transport
42 resulting in a mixed water-sediment flow (e.g. Outland 1963; Capart, 2000; Zech et al., 2009;
43 Goutiere et al., 2011). Further away from the dam, significant morphological changes to the
44 catchment can occur and in extreme cases, the morphology of the river and its surroundings can
45 be completely reshaped.

46 Thus to fully understand the consequences of dam break, measurements or numerical models of
47 sediment transport rate must be considered along with dam break flow velocity. Field
48 observations are rare as they can be difficult, costly and dangerous to perform. Without field
49 observations, however, validating numerical models for real-world dam failures is problematic.
50 Thus, laboratory experiments, due to their relative simplicity, ease of control, and ability to
51 generate repeatable datasets (Howard 2008), play an important role in the development and
52 validation of these models. Over the last few decades, an abundance of laboratory experiments
53 on dam break flows over fixed beds have investigated velocity distributions, flood propagation
54 and water levels (e.g. Soares-Frazão & Zech 2002; Soares-Frazão 2007; Soares-Frazão & Zech
55 2008). Increasingly, the focus has turned towards experimental testing of mobile beds which
56 better reflect conditions found in natural rivers (e.g. Fraccarollo & Capart 2002; Leal et al. 2002;
57 Leal 2005; Spinewine & Zech 2007; McMulli, 2015). For example, Leal et al. (2002)
58 investigated dam break over uniform mobile sand beds in a flume and showed that bed sediment
59 mobility, initial downstream water depth and initial bed step height play important roles in the

60 behavior of sediments dislodged downstream of a dam. Soares-Frazão et al. (2012) conducted
61 similar experiments revealing that intense scour occurred near the failed dam and sediment
62 deposition was present further downstream. Qian et al. (2017) conducted a laboratory
63 investigation into the impact of partial dam break floods on bed topography and revealed that the
64 scour and deposition patterns observed in previous studies over uniform beds also occur over
65 non-uniform beds. The final bed surfaces showed a general coarsening trend in the intense scour
66 and deposition areas. In other parts of the reach, small bed-forms, that produced a coarse-fine-
67 coarse bed structure, were only observed in cases with non-uniform sediment.

68 Previous studies have only investigated the difference in temporal flow distributions and bed
69 evolution between uniform and non-uniform beds. To the best knowledge of the authors, no
70 other study has examined the effect of grain size uniformity on bed-load transport rates. This
71 study is a first attempt to fill this gap by experimentally investigating the impact of dam break
72 flows on bed-load transport rates over uniform and non-uniform sediments, with varying
73 reservoir water levels and downstream bed slopes.

74 **Methodology**

75 *Flume set-up*

76 The experiments were carried out using a 12 m long by 0.5 m wide flume with a depth of 0.5 m.
77 The dam break was simulated using a fast vertical PVC lift-gate that was installed 4.4 m from the
78 upstream end of the flume (Fig. 1 and Fig A1 in the Appendix). The first 3.4 m of the flume was
79 composed of fixed bed material and a 1 m long section immediately upstream of the gate was
80 constructed of mobile sediment. Downstream of the gate, a 5 m long mobile section was created
81 and two bed-load traps (each 0.15 m wide by 0.5 m long) were embedded at the end of this
82 section. The remaining 2.3 m of the flume was constructed of fixed bed material. The thickness
83 of the sediment sections was 6-8 d_{50} and the total volume of the reservoir was between 0.24 to
84 0.77 m^3 , where d_{50} is the median bed sediment diameter. Ultrasonic sensors, operating at 25 Hz,
85 measured water depth behind the gate at 4.30 m (Sensor 1) and downstream of the gate at
86 distances of 4.90 m (Sensor 2) and 5.90 m (Sensor 3). Three digital cameras were installed: one
87 at the gate location to calculate the opening time of the gate, a second at the end of the movable
88 bed to record the arrival time of the flood wave, and a third camera at the two bed-load traps to

89 measure the time taken for the traps to be filled. The opening times of the gate (from 0.15 to 0.25
90 s) reveal that the simulated dam breaks can be considered to have occurred instantaneously
91 (Lauber & Hager 1998).

92
93

94 ***Experimental procedure***

95 Four uniform gravel mixtures with mean diameters of 5.17, 10.35, 14.0 and 20.7 mm were
96 investigated, as well as a non-uniform mixture with d_{50} of 12.5 mm and sorting coefficient (σ_g) of
97 1.7 that was composed of these four uniform sediments in equal weight proportions (Table 1).
98 Each experiment was performed using a static reservoir water level (h_1) of either 0.15, 0.20 or
99 0.35 m upstream of the gate. A water depth of 0.01 m (h_0) was allowed to form downstream of
100 the gate and was kept uniform for all experiments through the use of a downstream weir. Before
101 beginning the experiments, the water level behind and downstream of the dam was set using
102 ultrasonic sensors and point gauges. No sediment feed was used due to the very short duration of
103 each experiment (between 8 to 25 s). To investigate the impact of bed slope on bed-load
104 transport, a total of eight longitudinal slopes (S), ranging from 0.005 to 0.035, were used (Table
105 2). A photo of the flume (Fig. A1), an example of a hydrograph (Fig. A2) and changes in the
106 sediment bed resulting from a dam break (Fig. A3) are presented in the Appendix. The flow
107 unsteadiness was high due to rapid changes in the hydrograph. Thus there is uncertainty in the
108 estimate of bed shear velocity (Mrokowska, & Rowinski, 2019). Sources of uncertainty include
109 the movement of bed sediment affecting fluid momentum (Carbonneau & Bergeron, 2000) and a
110 high level of ambiguity in defining the datum and bed shear velocity in a mobile bed (Nikora et
111 al., 2007; Ferreira et al., 2012).

112

113 ***Dimensionless bed-load parameter***

114 After each run, the transported sediment collected in the bed-load traps was dried, sieved and
115 weighed fractionally. Using these samples, the bed-load transport rate was calculated and used to
116 estimate the dimensionless bed-load parameter for the uniform (q_s^*) and non-uniform mixtures
117 (q_{si}^*) [-]:

118

$$q_s^* = \frac{q_s}{\rho_s \sqrt{(s-1)gd^3}}, q_{si}^* = \frac{q_{si}}{f_i \rho_s \sqrt{(s-1)gd_i^3}} \quad (1)$$

where q_s is the bed-load transport rate of the uniform sediment [$\text{kg m}^{-1}\text{s}^{-1}$], q_{si} is the fractional sediment transport rate [$\text{kg m}^{-1}\text{s}^{-1}$], d is the mean size of the uniform sediment [m], d_i is the mean of the grain size fraction i [m], f_i is the proportion of fraction i in the bed surface [-], g is gravitational acceleration [m s^{-2}], ρ_s is the sediment density [kg m^{-3}], $s = \rho_s / \rho_w$ is the relative density of sediment [-] and ρ_w is water density [kg m^{-3}].

125 ***Impact factor***

126 To assess the difference in the mobility of a non-uniform grain size fraction with its equivalent in
127 a uniform sediment, the impact factor F_i was estimated (Li et al., 2016):

$$F_i = \left(\frac{q_{si}}{f_i} \right) / \left(\frac{q_s}{f} \right) \quad (2)$$

130 where f is the proportion of the uniform sized sediment in the bed surface [-] and thus is equal to
131 1. The finer fractions in a non-uniform mixture may be hidden by the coarser fractions, and thus,
132 have an impact factor of less than 1. The converse is likely to be the case for the coarser fractions
133 and thus they would have an impact factor greater than 1. If the mobility of a fraction in a non-
134 uniform mixture is equal to the mobility of a uniform-sized counterpart, the impact factor is
135 equal to unity.
136

137

138 **Result and discussion**

139

140 ***Difference in bed-load transport of uniform and non-uniform sediment***

141 At a slope of 0.01, there was no transport of non-uniform sediment; however, there was active
142 transport of uniform bed sediments of 5.17, 10.35 and 14.0 mm. This result implies that non-
143 uniform bed material was more stable than the fine uniform bed sediments because of the
144 presence of a 20.7 mm fraction. A comparison between the 14.0 mm fraction in the non-uniform
145 sediment and its uniform sediment counterpart shows that the uniform sediment had a higher

146 dimensionless bed-load parameter than the non-uniform sediment (Fig. 2a). At reservoir water
147 levels of 0.12, 0.20 and 0.35 m with a slope of 0.02, the bed-load parameter for 14.0 mm uniform
148 sediments was 71 %, 35 % and 27 % higher than for the counterpart non-uniform fraction,
149 respectively. For the coarser fraction of 20.7 mm, the relation was reversed; at a slope of 0.03 the
150 bed-load parameter was 26 %, 38 % and 17 % higher for the 20.7 mm non-uniform fraction than
151 for the counterpart uniform sediment, respectively (Fig. 2b). This result is attributed to protrusion
152 and hiding effects that exist in non-uniform sediments which enhance the mobility of coarser
153 fractions and decrease the mobility of finer fractions. These effects are confirmed by the
154 transported sediment being coarser than the initial sediment in the flume (Fig. 3).

155 To further highlight the impact of the finer fractions of the non-uniform sediments on the
156 mobility of the coarser fractions, the fractional transport rate of the 14.0 mm (F14) and 20.7 mm
157 (F20.7) fractions were compared to the rate of their uniform counterparts (Fig. 4). The results
158 reveal that the 20.7 mm fraction was more mobile, while the 14.0 mm fraction was less mobile.
159 This finding implies that the finer fractions in the non-uniform sediment caused the coarser
160 fractions to be more easily eroded. Furthermore, the 14.0 mm fraction was less susceptible to
161 erosion. These results are in accordance with those for steady (Li et al., 2016) and gradually
162 varied flow conditions (Li et al., 2018). Figure 4 also shows that when the reservoir water level
163 increased, the relative fractional rates tended towards one. Only at lower water levels and lower
164 levels of hydraulic energy did protrusion and hiding effects become apparent. This result is also
165 in accordance to previous findings for uniform flow conditions (Li et al., 2016).

166

167 ***Effect of reservoir water level on bed-load transport of non-uniform sediment***

168 The change in the bed-load parameter of the non-uniform fractions with reservoir water level is
169 shown in Figure 5 for three bed slopes. This figure shows that, for water levels of 0.12 and 0.20
170 m, the bed-load parameter of the finer fractions (5.17 and 10.35 mm) was higher than the coarser
171 fractions (14.0 mm and 20.7 mm). The opposite trend was observed at a water level of 0.35 m.
172 For example, with a slope of 0.02, the bed-load parameter for the finest fraction was 6.53 and
173 2.45 times higher than for the coarsest fraction at water levels of 0.12 and 0.20 m, respectively.
174 For the water level of 0.35 m, at the same bed slope, the bed-load parameter for the coarsest
175 fraction was 1.65 higher than for the finest fraction. These differences in mobility of the fine and

176 coarse fractions with reservoir water level are likely to have occurred due to difference in shear
177 stress. At the highest water level, there was sufficient force for the transportation of both coarse
178 and fine fractions. Thus, the effect of enhanced protrusion of the coarse grains was apparent,
179 causing the bed-load parameter for coarser fractions to be higher. In contrast, at the lower water
180 levels, the shear stress was not high enough to transport sufficient proportions of coarse-grained
181 sediment, thus the effects of enhanced protrusion on the mobility of the coarse grains was not
182 observed. Thus overall, the effect of hiding and protrusion decreased with increasing water level.
183 These changes in mobility with reservoir water level were reflected in the grain sizes of the
184 transported sediments (Fig. 3); for slopes of 0.02 and 0.03, the median transported grain size
185 increased with reservoir water level from 12.5 to 19.5 mm, and from 14.5 to 19.6 mm,
186 respectively.

187 Future research should investigate further the effects of dam break flows on bed-load transport
188 over a wider range of non-uniform sediment mixtures, with differing d_{50} and sorting, and over
189 water-worked beds that better mimic the surface topographies of natural coarse-grained rivers
190 (Cooper and Tait 2009). In addition, there is a need to examine whether the relative mobility of
191 coarse and fine fractions differs between the rising and falling limb of a flood hydrograph (Wang
192 et al. 2015), and if the flood hydrograph resulting from dam breaks acts to transport non-uniform
193 mixtures in the same manner as unsteady flood hydrographs. Future studies should also focus on
194 quantifying the bed topography adjustments due to dam break flows in order to provide detailed
195 explanations for the changes in the mobility of non-uniform sediment fractions.

196 **Conclusion**

197 Laboratory experiments in a flume have quantified the mobility of non-uniform sized sediment
198 in dam break flows and how this differs from uniform-sized sediment. The dimensionless bed-
199 load parameter of the finer fractions of the non-uniform bed was lower than the same sized
200 material on a uniform bed, although the coarsest fraction had a higher bed-load parameter. The
201 finer fractions were more stable, and the coarser fractions were more erodible in graded bed
202 sediment compared to a uniform-grained bed. By investigating changes in mobility of the mixed-
203 size fractions with reservoir water levels, the results revealed that at low water levels, when the
204 coarser fractions were only just mobile, the bed-load parameter of the finer fractions was higher

205 than the coarser fractions. The opposite was observed at a higher water level when a significant
206 proportion of the coarsest fractions were mobilized, and the higher protrusion of these grains had
207 an important impact on their mobility relative to the finer grains. The transported sediment in
208 these mixed sized beds was coarser than the initial bed sediment, and became coarser with an
209 increase in reservoir water level.

210 **References**

- 211 Bombar, G., Elci, S., Tayfur, G., Guney, M.S., & Bor, A. (2011). Experimental and numerical
212 investigation of bed-load transport under unsteady flows, *Journal of Hydraulic Engineering*,
213 137, 1276-1282.
- 214 Bozkus, Z. (2004). Dam break analysis for disaster management, *IMO Teknik Dergi*, 15, 3335-
215 3350 (in Turkish).
- 216 Capart, H. (2000). Dam-break induced geomorphic flows and the transition from solid- to fluid-
217 like behaviour across evolving interfaces, *PhD thesis*. UCL, Belgium.
- 218 Carbonneau, P.E., & Bergeron, N.E. (2000). The effect of bedload transport on mean and
219 turbulent flow properties, *Geomorphology*, 35, 267-278,
- 220 Cooper, J.R., & Tait, S.J. (2009). Water-worked gravel beds in laboratory flumes - a natural
221 analogue?, *Earth Surface Processes and Landform*, 34, 384-397, doi:10.1002/esp.1743.
- 222 Ferreira, R.M.L., Franca, M.J., Leal, J.G.A.B., & Cardoso, A.H. (2012). Flow over rough mobile
223 beds: Friction factor and vertical distribution of the longitudinal mean velocity, *Water*
224 *Resources Research*., 48, <https://doi.org/10.1029/2011WR011126>.
- 225 Fraccarollo, L., & Capart, H. (2002). Riemann wave description of erosional dam-break flows,
226 *Journal of Fluid Mechanics*, 461, 183–228, doi:10.1017/S0022112002008455
- 227 Goutière, L., Soares-Frazão, S., & Zech, Y. (2011). Dam-break flow on mobile bed in abruptly
228 widening channel: Experimental data, *Journal of Hydraulic Research*, 49(3): 367–371.
229 doi:10.1080/00221686.2010.548969.
- 230 Howard H.C. (2008). River morphology and river channel changes, *Transactions of Tianjin*
231 *University*, 14: 254-262.
- 232 Tabarestani, M., & Zarrati, A. (2015). Sediment transport during flood event: a review,
233 *International Journal of Environmental Science and Technology*, 12, 775-788 doi:
234 10.1007/s13762-014-0689-6.

235 Lauber, G., & Hager, W.H. (1998). Experiments to dam break wave: Horizontal channel,
236 *Journal of Hydraulic Research*, 36, 291–307, doi:10.1080/00221689809498620.

237 Leal, J.G.A.B., Ferreira, R.M.L., & Cardoso, A.H. (2002). Dam-break waves on movable bed. In
238 *D. Riverflow, Proceedings of the 1st IAHR International Conference on Fluvial Hydraulics*,
239 Balkema, Rotterdam, The Netherlands, 981-990.

240 Leal, J.G.A.B. (2005). Experimental and mathematical modeling of dam-break waves over
241 mobile bed open channels, *PhD thesis, Universidade da Beira Interior, Covilhã* (in
242 Portuguese).

243 Li, Z., Cao, Z., Liu, H., & Pender, G. (2016). Graded and uniform bed-load sediment transport
244 in a degrading channel, *International Journal of Sediment Research*, 31, 376-385, doi:
245 10.1016/j.ijsrc.2016.01.004.

246 Li, Z., Qian, H., Cao, Z., Liu, H., Pender, G., & Hu, P. (2018). Enhanced bed load sediment
247 transport by unsteady flows in a degrading channel, *International Journal of Sediment*
248 *Research.*, 33., 327-339, <https://doi.org/10.1016/j.ijsrc.2018.03.002>.

249 McMullin, N. (2015). Numerical and experimental modelling of dam break interaction with a
250 sediment bed, *PhD thesis, University of Nottingham*.

251 Molu, M. (1995). Dam break flood in a natural channel: A case study, *MSc thesis, Civil*
252 *engineering Department, Middle East Technical University, Ankara, Turkey*.

253 Mrokowska, M.M., & Rowinski, P.M. (2019). Impact of unsteady flow events on bedload
254 transport: A review of laboratory experiments, *Water*, 11, 907; doi:10.3390/w11050907.

255 Nikora, V., McEwan, I., McLean, S., Coleman, S., Pokrajac, D., & Walters, R. (2007) Double-
256 averaging concept for rough-bed open-channel and overland flows: Theoretical background,
257 *Journal Hydraulic Engineering*, 133, 873–883.

258 Outland, C. F. (1963). *Man-made disaster: The story of St. Francis Dam*, The Arthur H. Clark
259 Company, Glendale.

260 Qian, H., Cao, Z., Liu, H., & Pender, G. (2017). New experimental dataset for partial dam break
261 floods over mobile beds, *Journal of Hydraulic Research*, 56, 124-135.
262 <http://dx.doi.org/10.1080/00221686.2017.1289264>.

263 Redolfi, M., Bertoldi, W., Tubino, M., & Welber, M. (2018). Bed load variability and
264 morphology of gravel bed rivers subject to unsteady flow: A laboratory investigation, *Water*
265 *Resources Research*, 54, 842–862.

266 Soares-Frazão, S. (2007). Experiments of dam-break wave over a triangular bottom sill, *Journal*
267 *of Hydraulic Research*, 45, 19-26, doi:10.1080/00221686.2007.9521829.

268 Soares-Frazão, S., & Zech, Y. (2008). Dam-break flow through an idealized city, *Journal of*
269 *Hydraulic Research*, 46, 648–658, doi:10.3826/jhr.2008.3164

270 Soares-Frazão, S., & Zech, Y. (2002). Dam break in channels with 90° bend, *Journal of*
271 *Hydraulic Engineering*, 128: 956–968, doi:10.1061/(ASCE)0733-9429(2002)128:11(956).

272 Soares-Frazão, S., Canelas, R., Cao, Z., Cea, L., Chaudhry, H.M., Moran, A.D., & Zech, Y.
273 (2012). Dam-break flows over mobile beds: Experiments and benchmark tests for numerical
274 models. *Journal of Hydraulic Research*, 50 (4), 364–375.
275 doi:10.1080/00221686.2012.689682.

276 Spinewine, B., & Zech, Y. (2007). Small-scale laboratory dam-break waves on movable beds,
277 *Journal of Hydraulic Research*, 45,:73–86, doi:10.1080/00221686.2007.9521834.

278 Stansby, P.K, Chegini, A., & Barnes, T.C.D. (1998). The initial stages of dam-break
279 flow.,*Journal of Fluid Mechanics*. 374: 407-424.

280 Wang, L., J.S., Cuthbertson, A., Pender, G., & Cao, Z. (2015). Experimental investigations of
281 graded sediment transport under unsteady flow hydrographs, *International Journal of*
282 *Sediment Research*, 30, 306-320.

283 Table 1. Physical properties of bed sediments, where d_{50} is the median grain size of the mixture,
 284 σ_g is the sorting coefficient, d is the mean grain size, ρ_s is the sediment density and Φ is porosity
 285

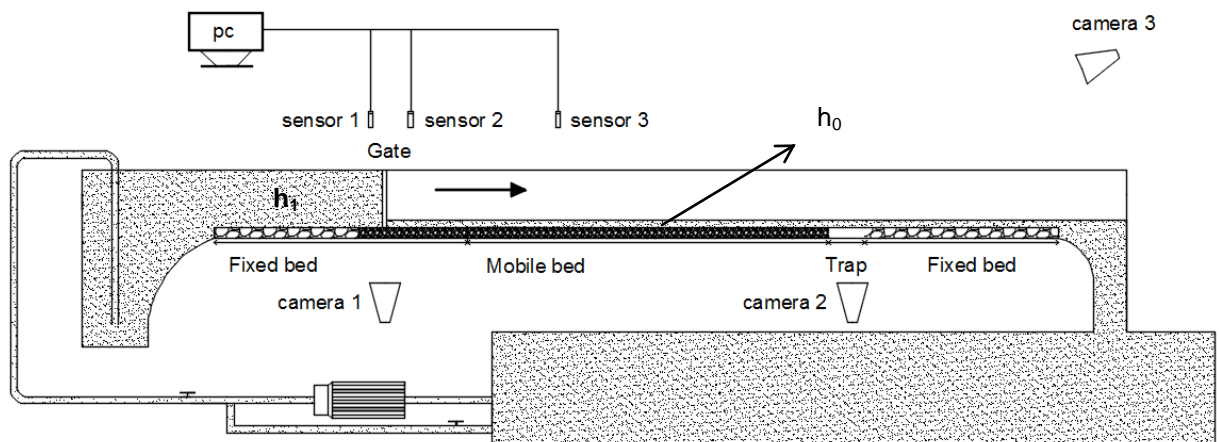
Sediment	Fraction [mm]	d_{50} [mm]	σ_g [-]	d [mm]	ρ_s [kg/m ³]	Φ [-]
Fine gravel	4.75-5.6	-	-	5.17	2391	0.4
Lower medium gravel	9.5-11.2	-	-	10.035	2375	0.4
Higher medium gravel	13-15	-	-	14	2900	0.45
Coarse gravel	19-22.4	-	-	20.7	2552	0.43
Graded (mixture)	4.75-22.4	12.5	1.7	13.57	2567	0.37

286
 287
 288
 289
 290
 291
 292
 293
 294
 295
 296
 297
 298
 299
 300

301 Table 2. Summary of the experimental conditions, where d is the mean grain size, S is the flume
 302 slope, h_1 is the reservoir water level, q_s is the bed-load transport rate and q_s^* is the dimensionless
 303 bed-load parameter.

d [mm]	S [-]	Run code	h_1 [m]	q_s [$\text{kg m}^{-1} \text{s}^{-1}$]	q_s^* [-]
5.17	0.005	A-1	0.12	0.07	0.02
		A-1	0.20	1.04	0.23
		A-1	0.35	1.14	0.34
	0.0075	A-2	0.12	0.57	0.17
		A-2	0.20	0.78	0.28
		A-2	0.35	1.16	0.37
	0.01	A-3	0.12	0.82	0.24
		A-3	0.20	1.10	0.33
		A-3	0.35	1.66	0.51
10.35	0.01	B-1	0.12	0.41	0.045
		B-1	0.35	3.62	0.39
14	0.01	C-1	0.12	0.29	0.014
		C-1	0.20	0.73	0.035
		C-1	0.35	1.12	0.055
	0.02	C-2	0.12	0.92	0.042
		C-2	0.20	1.09	0.053
		C-2	0.35	3.16	0.15
20.7	0.03	D-1	0.12	0.23	0.008
		D-1	0.20	0.88	0.03
		D-1	0.35	3.24	0.1
	0.0325	D-2	0.12	0.40	0.013
		D-2	0.20	0.95	0.033
		D-2	0.35	3.38	0.15
	0.035	D-3	0.12	0.51	0.017
		D-3	0.20	1.06	0.036
		D-3	0.35	4.83	0.17
Non-uniform	0.015	E-1	0.12	0.08	0.002
		E-1	0.20	0.42	0.017
		E-1	0.35	1.12	0.042
	0.02	E-2	0.12	0.14	0.01
		E-2	0.20	0.42	0.019
		E-2	0.35	1.61	0.058
	0.03	E-3	0.12	0.33	0.018
		E-3	0.20	1.13	0.058
		E-3	0.35	2.02	0.076

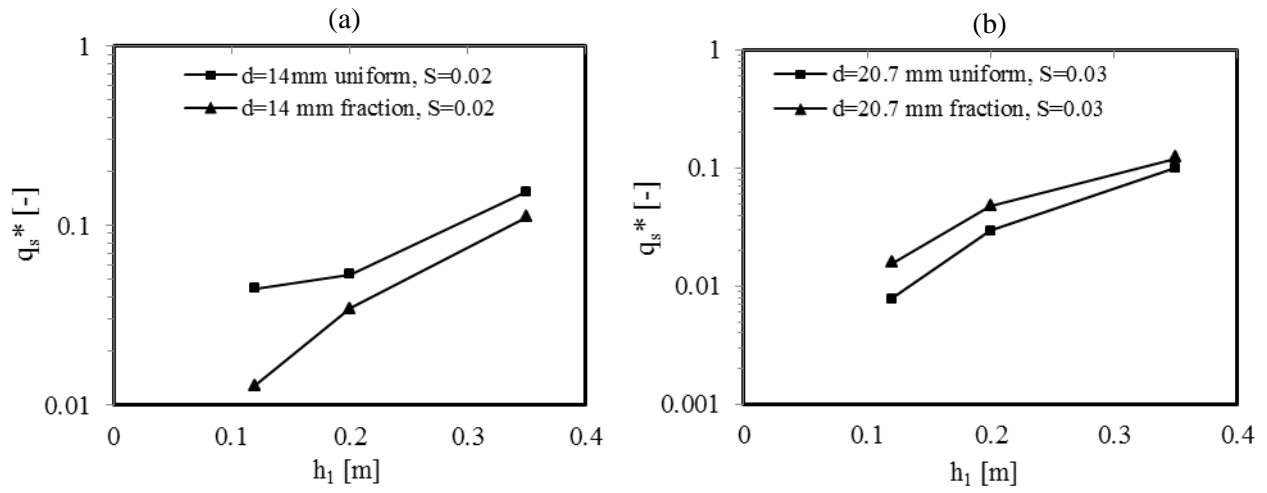
304



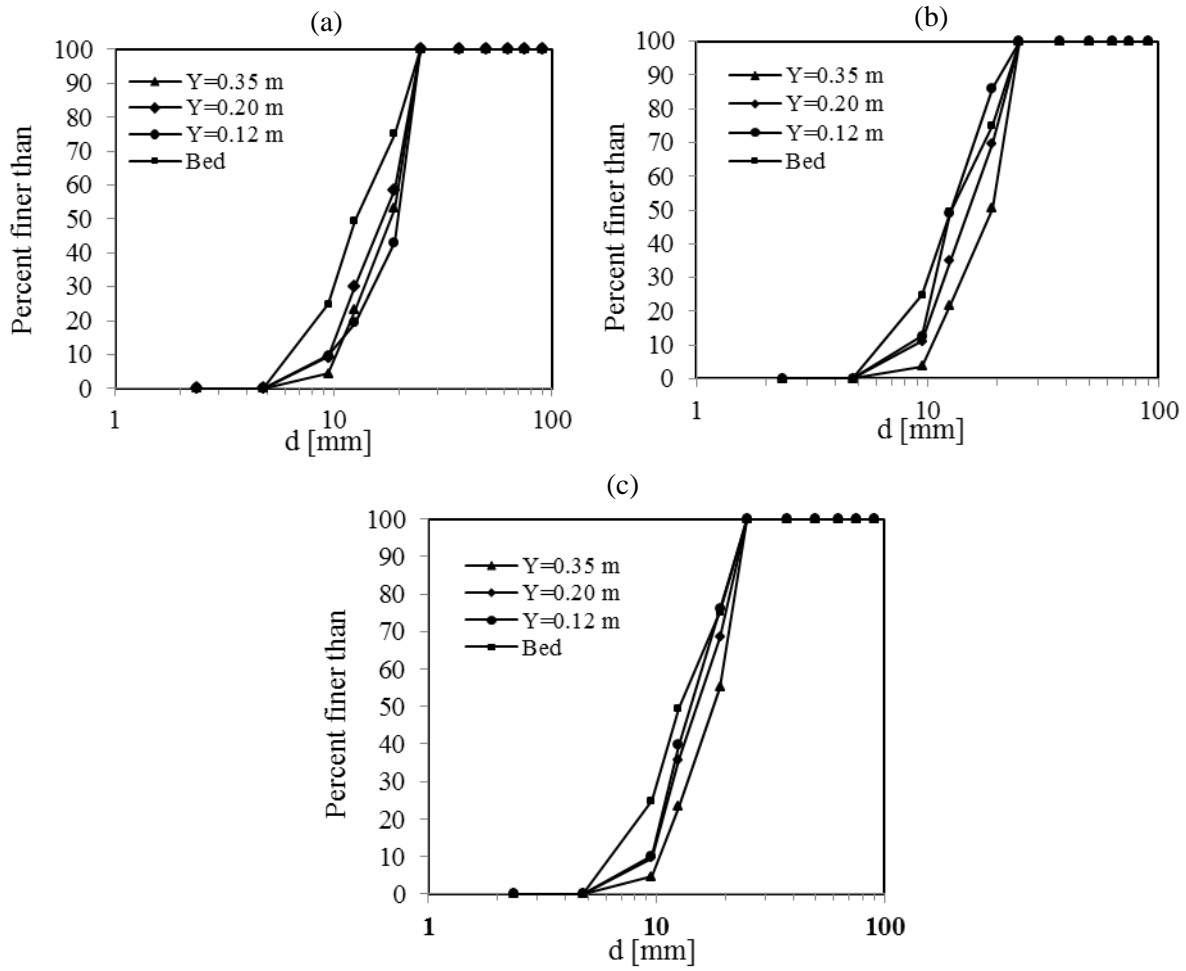
305

306

Fig. 1. Schematic of the flume (side view).



317 Fig. 2. Comparison of the dimensionless bed-load parameter (q_s^*) between the non-uniform
 318 fractions and uniform-sized counterparts at sizes of (a) 14 mm and (b) 20.7 mm.



326

327

328

329

330

331

332

333

334

335

336

337 Fig. 3. Grain size distributions of the initial bed sediment and the transported non-uniform sediment at
 338 slopes of (a) 0.015, (b) 0.02, and (c) 0.03.

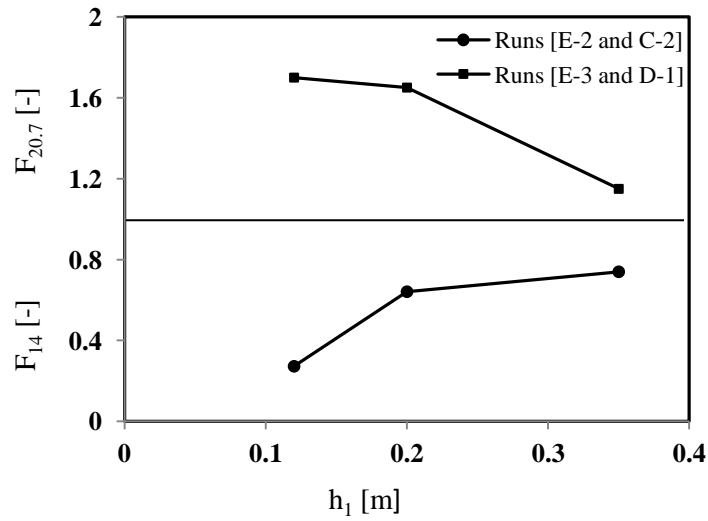
339

340

341

342

343



344

345

346

347

348

349 Fig. 4. Effect of reservoir water level (h_1) on the relative fractional sediment transport rate of two

350 non-uniform fractions, 14.0 mm (F_{14}) and 20.7 mm ($F_{20.7}$) at slopes of 0.02 and 0.03.

351

352

353

354

355

356

357

358

359

360

361

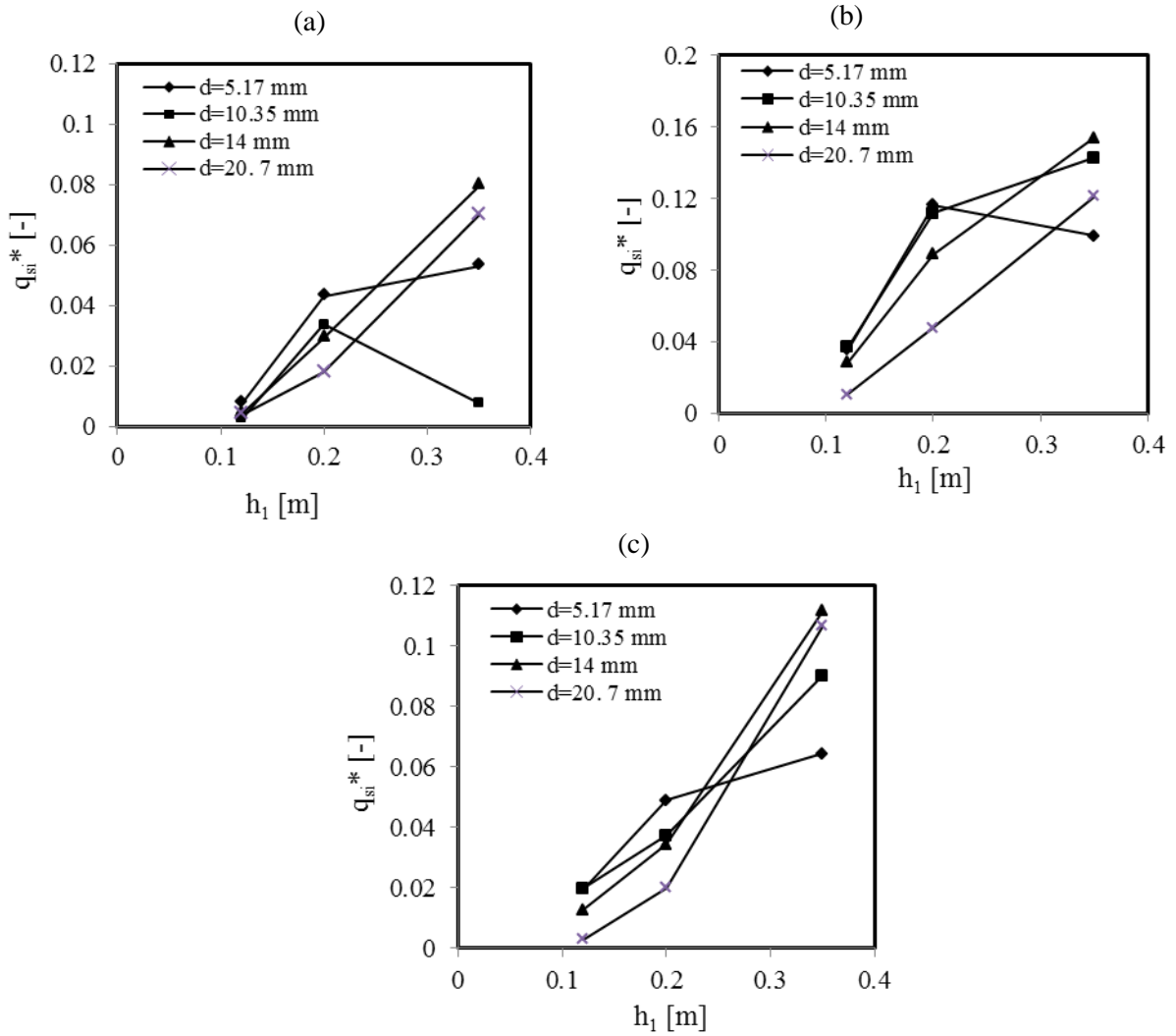
362

363

364

365

366



367 Fig. 5. Effect of reservoir water level (h_1) on the dimensionless bed-load parameter (q_{Si}^*) at
368 slopes of (a) 0.015, (b) 0.02 and (c) 0.03.

369

370 **Appendix**

371

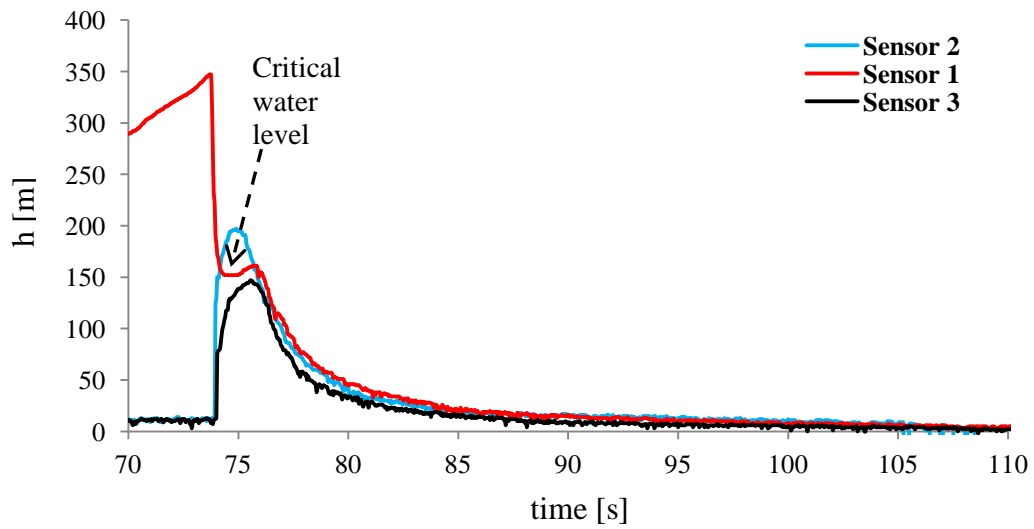


372

373 Fig A. The location of the dam and its reservoir in the flume.

374

375



376

377

378 Fig. B. Discharged hydrograph resulting from dam break (red-line shows the water depth h in the
379 reservoir, and the blue- and green-lines show the water depth at 0.5 m and 1.5 downstream of the
380 dam.

381



382

383

384

Fig. C. Bed morphology changes after a dam-break flow